Distinct molecular etiologies of male and female hepatocellular carcinoma

Heini M. Natri[1]*, Melissa A. Wilson[1], Kenneth Buetow[1]

[1] Center for Evolution and Medicine, School of Life Sciences, Arizona State University, Tempe, Arizona, USA

Corresponding author:

E-mail: hnatri@asu.edu (H.M.N)

Abstract

Sex-differences in cancer occurrence and mortality are evident across tumor types; men exhibit higher rates of incidence and often poorer responses to treatment. Targeted approaches to the treatment of tumors that account for these sex-differences require the characterization and understanding of the fundamental biological mechanisms that differentiate them. Hepatocellular Carcinoma (HCC) is the second leading cause of cancer death worldwide, with the incidence rapidly rising. HCC exhibits a male-bias in occurrence and mortality, but previous studies have failed to explore the sex-specific dysregulation of gene expression in HCC. Here, we characterize the sex-shared and sex-specific regulatory changes in HCC tumors in the TCGA LIHC cohort. By using sex-specific differential expression analysis of tumor and tumor-adjacent samples, we uncovered etiologically relevant genes and pathways differentiating male and female HCC. While both sexes exhibited activation of pathways related to apoptosis and p53 signaling, pathways involved in innate and adaptive immunity showed differential activation between the sexes. Using eQTL analyses, we discovered germline variants with differential effects on tumor gene expression between the sexes. 24.3% of the discovered eQTLs exhibit differential effects between the sexes, illustrating the substantial role of sex in modifying the effects of eQTLs in HCC. The genes that showed sex-specific dysregulation in tumors and those that harbored a sex-specific eQTL converge in clinically relevant pathways, suggesting that the molecular etiologies of male and female HCC are partially driven by differential genetic effects on gene expression. Overall, our results provide new insight into the role of inherited genetic regulation of transcription in modulating sex-differences in HCC etiology and provide a framework for future studies on sex-biased cancers.

Background

Differences in cancer occurrence and mortality between sexes are evident across tumor types; males exhibit higher rates of cancer incidence and often poorer response to treatment, including some forms of chemotherapy and immunotherapy [1,2]. While differences in risk factors may explain some portion of the sex-bias, the bias remains after appropriate adjustment for these factors [3,4]. A recent study examining the mutational profiles of tumors from males and females across The Cancer Genome Atlas (TCGA) found sex-differences in mutational profiles , calling for the consideration of sex as a biological variable in studies on cancer occurrence, etiology, and treatment [5]. Despite these underlying molecular differences, sex is rarely considered in the development of cancer therapies.

Across tumor types analyzed, the largest sex-differences in autosomal mutational profiles were seen in liver hepatocellular carcinoma (HCC), indicating that male and female HCC are etiologically distinct [5].

41 Furthermore, HCC exhibits sex-bias in occurrence, with a male-to-female incidence ratio between 1.3:1
42 and 5.5:1 across populations [6,7]. The sexes also differ in the clinical manifestation of HCC, males
43 exhibiting an earlier onset and more/larger nodules [8]. HCC is the second leading cause of cancer
44 mortality worldwide, accounting for 8.2% of all cancer deaths [2], and the incidence in the US has
45 doubled in the last 3 decades, attributable to increased rates of obesity [7], calling for the development of
46 new interventions and targeted therapies.

47 Sex-specific gene regulation may partially underlie differences between the sexes in disease prevalence
48 and severity [9,10]. Previous work observed extensive sex-biased signatures in gene expression in HCC
49 and other sex-biased cancers [11]. However, this study focused solely on comparing male and female
50 tumor samples, without consideration sex-differences in non-diseased and tumor-adjacent tissues. To
51 understand cancer-specific processes, it is necessary to contrast the sex-differences in gene expression
52 identified in HCC with those in non-tumor and tumor tissues. For the targeted treatment of tumors, it is
53 necessary to understand whether sex differences in cancer reflect unique cancer-specific changes, or are
54 reflective of healthy sex-differences that may underlie observed sex-bias in cancer occurrence and disease
55 etiology.

56 In addition to sex differences in overall gene expression due to the wide effects of sex as a biological
57 variable, genetic variants may alter gene expression in a sex-specific manner. A pan-cancer analysis of
58 the TCGA dataset identified 128 germline variants altering gene expression levels (eQTLs) in HCC [12].
59 However, this study purposefully controlled for and removed the effect of sex and, to date, a sex-specific
60 eQTL analysis in HCC has not been performed. Sex-stratified analyses can reveal sex-biased genetic
61 effects on gene expression that may be obscured in a joint analysis of both sexes - e.g. cases where the
62 regulatory variant has a zero or very small effect in one sex, or the eQTL exhibits an opposite effect
63 direction in the two sexes [13]. eQTLs that are discovered in one sex but not in the whole sample analysis
64 are likely to affect gene expression in a sex-dependent manner, and while a combined analysis of both
65 sexes achieves a greater statistical power to detect sex-shared effects, it dilutes the signal of sex-
66 dependent effects [14].

67 Targeted approaches to the treatment of male and female HCC require the characterization and
68 understanding of the fundamental biological mechanisms that differentiate them. Here, we analyzed data
69 from TCGA and The Genotype-Tissue Expression project (GTEx) to examine the sex-specific patterns of
70 gene expression and regulation in HCC. Here, we have contrasted the sex-biased patterns of gene
71 expression in HCC tumors with healthy and tumor-adjacent liver tissues, allowing us to detect sex-
72 differences in gene expression shared between and specific to the different tissues. We show that male

and female HCC exhibit differences in the dysregulation of genes and the germline genetic regulation of tumor gene expression. Importantly, these orthogonal approaches identify genes that converge in shared pathways, indicating sex-specific etiology in HCC. The results presented here have implications for the development of targeted therapies for male and female HCC.

Methods

Data

GTEx (release V6p) whole transcriptome (RNAseq) data (dbGaP accession #8834) were downloaded from dbGaP. TCGA LIHC Affymetrix Human Omni 6 array genotype data, whole exome sequencing (WES) and RNAseq data (dbGaP accession #11368) were downloaded from NCI Genomic Data Commons [15]. In total, RNAseq data from 91 male and 45 female GTEx donors, germline genotypes and tumor RNAseq data from 248 male and 119 female TCGA LIHC donors, as well as paired tumor and tumor-adjacent samples from 28 male and 22 female TCGA LIHC donors were utilized in this study. FASTQ read files were extracted from the TCGA LIHC WES BAM files using the *strip_reads*() function of *XYAlign* [16]. We used *FastQC* [17] to assess the WES and RNAseq FASTQ quality. Reads were trimmed using *TRIMMOMATIC IlluminaClip* [18], with the following parameters: seed mismatches 2, palindrome clip threshold 30, simple clip threshold 10, leading quality value 3, trailing quality value 3, sliding window size 4, minimum window quality 30 and minimum read length of 50.

Read mapping and read count quantification

Sequence homology between the X and Y chromosomes may cause the mismapping of short sequencing reads derived from the sex chromosomes and affect downstream analyses [16]. To overcome this, reads were mapped to custom sex-specific reference genomes using *HISAT2* [19]. Female samples were mapped to the human reference genome GRCh38 with the Y-chromosome hard-masked. Male samples were mapped to the human reference genome with Y-chromosomal pseudoautosomal regions hard-masked. Gene-level counts from RNAseq were quantified using *Subread featureCounts* [20]. Reads overlapping multiple features (genes or RNA families with conserved secondary structures) were counted for each feature.

Germline variant calling and filtering

BAM files were processed according to Broad Institute *GATK* (*Genome Analysis Toolkit*) best practices [21–23]: Read groups were added with *Picard Toolkit*'s *AddOrReplaceReadGroups* and optical

102 duplicates marked with *Picard Toolkit*'s *MarkDuplicates* (v.2.18.1,
103 http://broadinstitute.github.io/picard/). Base quality scores were recalibrated with *GATK* (v.4.0.3.0)
104 *BaseRecalibrator*. Germline genotypes were called from whole blood Whole Exome Sequence samples
105 from 248 male and 119 female HCC cases using the scatter-gather method with *GATK HaplotypeCaller*
106 and *GenotypeGVCFs* [21]. Affymetrix 6.0 array genotypes were lifted to GRCh38 using the UCSC
107 *LiftOver* tool [24] and converted to VCF. Filters were applied to retain variants with a minimum quality
108 score > 30, minor allele frequency > 10%, minor allele count > 10, and no call rate < 10% across all
109 samples.

110 Clinical characteristics and cellular content of tumor samples

111 Confounding effects, e.g. differences in clinical and pathological characteristics or cell type composition
112 of the sequenced samples, may contribute to the observed effect modification when utilizing stratified
113 analyses. We examined the differences in the clinical characteristics between males and females in the
114 TCGA LIHC cohort. We used a *t*-test to test for the equality of means in patient age and cell type
115 proportions, and Fisher's exact test to test to detect differences in risk factors and pathological
116 classifications (Supplementary Tables S1 and S2).

117 Filtering of gene expression data

118 FPKM (Fragments Per Kilobase of transcript per Million mapped reads) expression values for each gene
119 were obtained using *EdgeR* [25]. Each expression dataset was filtered to retain genes with mean
120 FPKM≥0.5 and read count of ≥6 in at least 10 samples across all samples under investigation. In the
121 comparative analysis of differentially expressed genes (DEGs) between the tumor vs. tumor-adjacent
122 samples in males, females, and both sexes, genes that reached the previously described expression
123 thresholds in at least one tissue in at least one sex were retained. This assures that the DEGs detected in
124 the sex-specific and combined analyses are not due to filtering.

125 Differential expression analysis

126 For differential expression (DE) analysis, filtered, untransformed read count data were quantile
127 normalized and logCPM transformed with *voom* [26]. From the TCGA LIHC dataset, paired tumor and
128 tumor-adjacent samples were available for 22 females and 28 males. From the GTEx liver dataset, 91
129 male and 45 female samples were used in the DE analysis. A multi-factor design with sex and tissue type
130 as predictor variables were used to fit the linear model. *duplicateCorrelation* function was used to
131 calculate the correlation between measurements made between tumor and tumor-adjacent samples on the

132 same subject, and this inter-subject correlation was accounted for in the linear modeling. As the paired
133 tumor samples differed significantly between the sexes in terms of race, tumor grade, and HBV status,
134 (Supplementary Tables S1 and S2), these parameters were included in the linear models as covariates.
135 Due to missing values in the covariate data, the final numbers of sample pairs used in the analyses were
136 18 females and 26 males.

137 DEGs between comparisons were identified using the *limma*/*voom* pipeline [26] by computing empirical
138 Bayes statistics with *eBayes*. An FDR-adjusted *p*-value threshold of 0.01 and an absolute $\log_2$ fold-change
139 (FC) threshold of 2 were used to select significant DEGs.

140 To reliably detect genes that are expressed in a sex-biased way in HCC but not in non-diseased liver or in
141 tumor-adjacent tissue, we examined genes that were DE in the male vs. female tumor comparison using
142 the previously described significance thresholds, but not in the male vs. female comparisons of normal or
143 tumor-adjacent samples with a relaxed significance threshold of FDR-adjusted *p*-value ≤ 0.1 and absolute
144 $\log_2(FC) \geq 0$.

145 To detect genes that are dysregulated in tumors compared to matched tumor-adjacent samples in each sex,
146 we identified DEGs in the tumor vs. tumor-adjacent comparison of males, females, and in the whole
147 sample. DEGs that were identified in one sex but not in the other or in the combined analysis of both
148 sexes were considered sex-specific. DEGs identified in the combined analysis were considered sex-
149 shared. This approach allows the identification of high-confidence sex-specific events that are a result of
150 the underlying biological differences as opposed to sampling or statistical power. ANOVA and Kruskal-
151 Wallis tests were used to test for equality of fold changes of sex-shared and sex-specific DEGs across
152 male, female, and all samples.

153 **Overrepresentation of biological functions and canonical pathways**

154 We further analyzed the sex-shared and sex-specific tumor vs. tumor-adjacent DEGs as well as the sex-
155 specific eQTL target genes (eGenes) to identify sex-shared and sex-specific pathways driving HCC
156 etiology. We used the *NetworkAnalyst* webtool [27], which utilizes a hypergeometric test to compute *p*-
157 values for the overrepresentation of genes in regards to GO terms and KEGG and Reactome pathways.
158 An FDR-adjusted *p*-value threshold of 0.01 was used to select significantly overrepresented GO terms
159 and canonical pathways.

160 **Accounting for confounding effects and population structure**

161 Gene expression values are affected by genetic, environmental, and technical factors, many of which may
162 be unknown or unmeasured. Technical confounding factors introduce sources of variance that may greatly
163 reduce the statistical power of association studies, and even cause false signals [28]. Thus, it is necessary
164 to account for known and unknown technical confounders. This is often achieved by detecting a set of
165 latent confounding factors with methods such as principal component analysis (PCA) or Probabilistic
166 Estimation of Expression Residuals (PEER) [29]. These surrogate variables are then used as covariates in
167 downstream analyses. We derived 10 PEER factors from the filtered tumor gene expression data, and
168 used the weights of these factors as covariates in the eQTL analysis. We used the R package *SNPRelate*
169 [30] to perform PCA on the germline genotype data. We accounted for population structure by applying
170 the first three genotype PCs as covariates in the eQTL analysis.

171 **eQTL analysis**

172 We used eQTL analyses to detect germline genetic effects on tumor gene expression. Similar to the DE
173 analysis, we utilized combined and sex-stratified analyses to detect sex-shared and sex-specific effects.
174 Germline genotypes and tumor gene expression data from 248 male and 119 female donors in the TCGA
175 LIHC cohort were used in the eQTL analysis. Filtered count data was normalized by fitting the FPKM
176 values of each gene and sample to the quantiles of the normal distribution. To account for technical
177 confounders and population structure, 10 *de novo* PEER factors and three genotype principal components
178 were used as covariates. *Cis*-acting (proximal) eQTLs were detected by linear regression as implemented
179 in *QTLtools* v.1.1 [31]. Variants within 1Mb of the gene under investigation were considered for testing.
180 We used the permutation pass with 10,000 permutations to get adjusted *p*-values for associations between
181 the gene expression levels and the top-variants in *cis*: first, permutations are used to derive a nominal *p*-
182 value threshold per gene that reflects the number of independent tests per cis-window. Then, *QTLtools*
183 uses a forward–backward stepwise regression to determine the best candidate variant per signal [31].
184 FDR-adjusted *p*-values were calculated to correct for multiple phenotypes tested, and an adjusted *p*-value
185 threshold of 0.01 was used to select significant associations. To allow the comparison of effect sizes of
186 sex-specific and sex-shared eQTLs across the sexes, effects of each variant located within the 1Mb *cis*-
187 window were obtained using the *QTLtools* nominal pass.

188 Similarly to the tumor vs. tumor-adjacent DEGs, eQTLs that were detected in one sex but not in the other
189 or in the combined analysis were considered sex-specific, while eQTLs detected in the combined analysis
190 were considered sex-shared. ANOVA and Kruskal-Wallis tests were used to test for equality of effect
191 sizes of sex-shared and sex-specific eQTLs across male, female, and all samples.

192 **Estimating statistical power in the eQTL analysis**

193 We used the R package *powereQTL* [32] to estimate the effect of the sample size to the statistical power
194 to detect eQTLs in the combined analysis of both sexes and in the sex-specific analyses (Fig. S2).

195 **Genomic annotations of eQTLs**

196 We used the R package *Annotatr* to annotate the genomic locations of eQTLs [33]. Variant sites were
197 annotated for promoters, 5'UTRs, exons, introns, 3'UTRs, CpGs (CpG islands, CpG shores, CpG shelves),
198 and putative regulatory regions based on ChromHMM [34] annotations.

199 **Results**

200 **Sex-specific patterns of gene expression in HCC**

201 We identified sex-differences in gene expression in non-diseased liver (GTEx; 21 sex-biased genes with
202 an FDR-adjusted *p*-value ≤ 0.01 and an absolute $\log_2 FC \geq 2$), tumor-adjacent tissue (TCGA LIHC; 21
203 genes), and HCC (TCGA LIHC; 53 genes) to characterize the shared and unique sex-differences that may
204 drive the observed sex-biases in HCC occurrence and etiology (Fig. 1, Supplementary Tables S3-5). X-
205 linked *XIST* and Y-linked genes were expressed in a sex-biased way across all tissues. While sex-biased
206 gene expression in non-diseased and tumor-adjacent tissues may contribute to the sex-differences in
207 cancer occurrence, sex-biased expression in tumors is suggestive of distinct molecular etiologies of male
208 and female HCC. We identified 34 genes that show sex-differences in expression in HCC, but not in
209 tumor-adjacent tissue or non-diseased liver, even with a relaxed significance threshold (Fig. 1A). Notably,
210 Notch-regulating *DTX1* (Fig. 1B) and signal transducer *CD24* were downregulated in male HCC.

211 To further examine the sex-shared and sex-specific mechanisms driving HCC etiology, we detected DEGs
212 between tumor and tumor-adjacent samples in males and females, as well as in the combined analysis of
213 both sexes. Dimensionality reduction of gene expression data shows that variation among the tumor and
214 tumor-adjacent samples is driven by tissue type and sex (Fig. 1C). When inspecting the tumor samples
215 only, the first dimension is largely driven by sex (Supplementary Fig. S1). In the combined analysis of
216 male and female samples, we detected 691 tumor vs. tumor-adjacent DEGs (Supplementary Table S6). In
217 male- and female-specific analyses, we detected 715 and 542 tumor vs. tumor-adjacent DEGs,
218 respectively (Supplementary Tables S7 and S8). Out of the total of 903 unique DEGs, 76.5% were shared
219 between the sexes. We identified 103 female-specific and 108 male-specific tumor vs. tumor-adjacent
220 DEGs. Notably, substantially more DEGs were detected in sex-specific analyses than in the unstratified

221 analysis (Fig. 1D). Specifically, DEGs that showed different magnitudes in fold change between the sexes
222 (based on ANOVA/Kruskal-Wallis tests) were detected in the sex-specific analyses (Fig. 2C, 2D), while
223 DEGs with similar fold changes across all comparisons were detected in the combined analysis as well as
224 the sex-specific analyses (Fig. 2A). Sex-shared DEGs that were only detected in the combined analysis,
225 and not in the sex-specific analyses, showed a large variance in expression and, due to limited power,
226 were not detected as statistically significant DEGs in sex-specific analyses (Fig. 2B). Tumor-infiltrating
227 immune cells may produce spurious signals in DE analyses, which is evident from the detection of
228 various immunoglobulin genes in tumor vs. tumor-adjacent comparisons (Supplementary Tables S6-8).
229 However, male and female samples did not significantly differ in terms of cellular content
230 (Supplementary Table S2), and thus such spurious signals are unlikely to affect male-female comparisons.
231 The observed differences in gene expression are thus likely to reflect actual sex-differences rather than
232 confounding differences in sample characteristics or composition.

233 To put these results in a broader context, we analyzed the male- and female-specific DEGs (tumor vs.
234 tumor-adjacent) for the overrepresentation of functional pathways. We found that the sex-shared and sex-
235 specific DEGs were enriched in pathways relevant to oncogenesis and cancer progression (Supplementary
236 Tables 9-11). We identified pathways that were overrepresented in only one of the sexes but not in the
237 other or in the combined analysis of both sexes, indicating that male and female HCC are partially driven
238 by different mechanisms and processes (Fig. 1E-F).

239 **Differential cis-eQTL effects in male and female HCC**

240 To further investigate the mechanisms of sex-difference in HCC etiology, we used eQTL analyses to
241 detect germline genetic effects on tumor gene expression in both the joint and sex-stratified analyses (Fig.
242 3A). We detected 1,204, 761, and 245 eQTLs in the combined, male-specific, and female-specific
243 analyses, respectively (Supplementary Tables S12-14). As expected, genomic annotations show that most
244 eQTLs are located on non-coding regions (Fig. 3B, Supplementary Tables S15-S17). Consistent with
245 previous reports, most *cis*-eQTLs were located near transcription start sites (TSSs), with 63% of all
246 eQTLs across the combined and sex-specific analyses being located within 20kb of TSSs. On average,
247 384 variants were tested per gene. 31% of the unique shared and sex-specific cis-eQTLs in HCC were
248 also identified as eQTLs in the liver data in the GTEx project analysis release V7, indicating shared tissue
249 origin. Out of the total of 1,595 unique associations, 75.7% were shared between the sexes. We detected
250 295 male-specific and 92 female-specific eQTLs. Since these associations were not detected in the
251 unstratified analysis, they are likely not a result of differential power to detect associations due to
252 different sample sizes, but exhibit effect modification by sex. Sex-specific associations exhibited

253 differences in effect size between the sexes (based on ANOVA/Kruskal-Wallis tests, Fig. 4C, 4D), and
254 the sex-specific effect is diluted in the combined analysis (Fig. 4C, 4D). Sex-shared large effect eQTLs
255 were detected in sex-specific and combined analyses (Fig. 4A), and, due to the larger sample size, sex-
256 shared low-effect eQTLs are detected in the combined analysis only (Fig. 4B).

257 We detected 27 shared eGenes that were associated with independent variants in males and females. This
258 could be due to actual biological differences in gene regulation, or due to technical constraints, in
259 particular, missing genotypes in one sex affecting the permutation scheme to select the top-variant for
260 each target gene. To overcome this and to detect high confidence instances of differential gene regulation
261 between the sexes, we further examined the sex-shared and sex-specific eGenes: we found 24 genes that
262 are under germline regulatory control in only male HCC (Fig. 3C), including *POGLUT1*, which is an
263 essential regulator of Notch signaling (Fig. 3D). No genes were found to be associated with nearby
264 variants in females only, likely due to reduced power to detect associations in females (Supplementary
265 Fig. S2). Male-specific eGenes were overrepresented in pathways related to cell cycle, apoptosis, and
266 cancer (Supplementary Table S18). Concordant with previous studies [14,35], none of the male-specific
267 eGenes were differentially expressed between male and female HCC, indicating that the male-specific
268 eQTLs are not a result of differences in overall gene expression levels between males and females, but are
269 likely to arise from factors such as differential chromatin accessibility or transcription factor activity. The
270 observation that non of the sex-biased autosomal genes in tumors harbor significant *cis*-eQTLs
271 (Supplementary Table S19) also suggests that while sex-specific *cis*-eQTLs may contribute to differences
272 in variance, sex-biased gene expression is likely a result of *trans*-effects, e.g. sex-chromosomal effects on
273 autosomal gene expression, or, more widely, a result of sex as a biological variable, e.g. hormonal effects.

274 Discussion

275 Distinct molecular etiologies of male and female HCC

276 It is well established that patterns of gene expression vary between the sexes across different tissues.
277 Previous studies have confounded these differences with those which may be driving etiological
278 differences between male and female tumors. For example, Yuan et al. previously reported extensive sex-
279 biased signatures in gene expression in HCC and other strongly sex-biased cancers [11]. While they
280 identified immunity and cancer-associated enriched pathways based on sex-biased genes detected in HCC
281 tumors, their approach was limited as it did not include the examination of non-diseased liver nor tumor-
282 adjacent tissues. From the results presented here, we are able to distinguish the differences detected in
283 comparisons of male and female HCC from those reflecting sex-differences in the healthy liver or in

284 tumor-adjacent tissue, as well as to detect genes that are dysregulated in HCC in a sex-shared or sex-
285 specific manner.

286 We characterized differences in gene expression between male and female HCC cases. Notably, sex-
287 differences in gene expression were the largest in the tumor tissue, with 53 genes (including 32 autosomal
288 genes) being expressed in a sex-biased way. These sex-differences point to distinct mechanisms
289 underlying HCC oncogenesis between the sexes, and may partially underlie the observed sex-biases in
290 HCC occurrence and onset. We detected 34 genes that were expressed in a sex-biased way in HCC
291 tumors, but not in healthy or tumor-adjacent liver tissues. Some of these genes are of particular interest in
292 the context of HCC: Notch-regulating *DTX1*, found here to be underexpressed in males compared to
293 females, has been identified as a putative tumor suppressor gene in head and neck squamous cell
294 carcinoma [36]. Another female-biased gene detected here, *CD24*, has a crucial role in T cell homeostasis
295 and autoimmunity [37]. The opposing roles of *CD24* expression in cancer and autoimmune diseases raise
296 interesting questions on the role of sex-differences in immunity underlying sex-differences in cancer.
297 Future studies will focus on better understanding the differential regulation of immune functions between
298 the sexes, and how these differences contribute to the observed biases in disease occurrence and etiology.

299 By sex-specific analyses of matched tumor and tumor-adjacent samples, we detected genes that are
300 uniquely dysregulated in male and female HCC. Further examination of these genes revealed sex-
301 differences in the pathway activation, indicating that the molecular etiologies of male and female HCC
302 are partly driven by distinct functional pathways. Males and females differed in the activation of several
303 signaling pathways, with females showing PPAR pathway enrichment while males showed PI3K,
304 PI3K/AKT, FGFR, EGFR, NGF, GF1R, Rap1, DAP12, and IL-2 signaling pathway enrichment (Fig. 1E,
305 Supplementary Tables 9-10). As these signaling pathways are notable targets for anti-cancer and anti-
306 metastasis therapies [38–44], the results presented here have implications for the targeted treatment of
307 male and female HCC.

308 Sex-specific germline genetic effects on tumor gene expression may drive the molecular 309 etiologies of male and female HCC

310 Sex-specific regulatory functions may underlie sex-differences in cancer etiology, progression, and
311 outcome. We detected sex-differences in the germline genetic regulation of tumor gene expression in
312 HCC, including 24 genes that were under germline regulatory control only in male HCC (Fig. 3).
313 Functional annotations of these male-specific eGenes provide insight into possible regulatory mechanisms
314 contributing to the observed male-bias in HCC and sex-differences in HCC etiology. Protein O-

315 glucosyltransferase 1 (*POGLUT1*) was found to be under germline regulation in male HCC, but not in
316 female HCC or in the joint analysis of both sexes (Fig. 3D). The eQTL associated with *POGLUT1* is
317 located on a promoter region of its target (Supplementary Table S15). *POGLUT1* is an enzyme that is
318 responsible for O-linked glycosylation of proteins. Altered glycosylation of proteins has been observed in
319 many cancers [45,46], including liver cancer [47,48]. *POGLUT1* is an essential regulator of Notch
320 signaling and is likely involved in cell fate and tissue formation during development. Genes involved in
321 Notch and PI3K/AKT signaling were also found to be expressed in a sex-biased way in HCC tumors and
322 overrepresented among the male-specific DEGs detected in the tumor vs. tumor-adjacent comparison,
323 showing that sex-specific eQTLs and sex-specific dysregulated genes converge in canonical pathways.
324 Notch signaling pathway was also detected as overrepresented (FDR-adj. p-value ≤ 0.01) among the 24
325 male-specific eGenes. PI3K-AKT is known to co-operate with Notch by triggering inflammation and
326 immunosuppression [49]. These results point to a major role of the Notch/PI3K/AKT axis in the
327 development of HCC in males. PI3K/AKT/mTOR signaling is of particular interest in the context of
328 HCC, as it has been implicated in HCC carcinogenesis [50], is involved in hepatic gluconeogenesis [51],
329 and is activated in a sex-biased way in liver and other tissues [52]. The role of Notch and PI3K/AKT
330 signaling in HCC may differ between early and late-stage tumors and among molecular subtypes, and
331 further studies are necessary to understand the possible oncogenic properties of these pathways among
332 HCC subtypes and between the sexes. In the future, analyses of data collected as a part of the
333 International Cancer Genomics Consortium project may elucidate the sex-specific processes of HCC
334 oncogenesis among the Japanese, as well as the interactions between sex and hepatitis infections in
335 shaping HCC etiology. However, each dataset has a unique ancestry composition and are not directly
336 comparable for validation purposes.

337 Conclusions

338 In summary, we discovered differential regulatory functions in HCC tumors between the sexes. This work
339 provides a framework for future studies on sex-biased cancers. Further studies are required to identify and
340 validate sex-specific genetic effects on tumor gene expression and its consequences in HCC and other
341 sex-biased cancers across diverse populations.

342 Abbreviations

343 HCC: Hepatocellular Carcinoma. HBV: Hepatitis B virus. HCV: Hepatitis C virus. DEG: Differentially
344 expressed gene. eQTL: Expression quantitative trait loci. TSS: Transcription start site.

Declarations

Acknowledgments

We thank Dr. Nicholas Banovich and anonymous reviewers for their feedback on previous versions of this manuscript.

Funding

This study was supported by ASU Center for Evolution and Medicine postdoctoral fellowship and the Marcia and Frank Carlucci Charitable Foundation postdoctoral award from the Prevent Cancer Foundation for HMN, ASU School of Life Sciences and the Biodesign Institute for startup funds for MAW, and ASU Center for Evolution and Medicine Venture funds.

Availability of data and materials

Data used in this study are available at dbGaP NCI Genomic Data Commons.

Authors' contributions

Conception and design: HMN, MAW, KB. Development of methodology: HMN, MAW. Acquisition of data: MAW, KB. Analysis and interpretation of data: HMN. Writing, review, and/or revision of the manuscript: HMN, MAW, KB. Study supervision: MAW, KB. All authors approved the final manuscript.

Ethics approval and consent to participate

Not applicable.

Consent for publication

Not applicable.

Competing interests

The authors declare no competing interests.

Additional files

Additional files contain supplementary information with two figures, and 19 supplementary tables.

368 **Fig S1.** A multi-dimensional scaling plot of the TCGA LIHC tumor samples of each sex (N male = 248,
369 N female = 119). Euclidean distances between samples were calculated based on 100 genes with the
370 largest standard deviations between samples.

371 **Fig S2.** Estimation of statistical power in the combined (grey), male-specific (blue), and female-specific
372 (red) eQTL analyses with a *p*-value level 0.01 and 384 variants. Increased power in the combined analysis
373 allows the detection of sex-shared low-effect eQTLs.

374 **Table S1.** Categorical clinical characteristics of male and female patients in the TCGA LIHC cohort.

375 **Table S2.** Continuous clinical characteristics of male and female patients in the TCGA LIHC cohort.

376 **Table S3.** Sex-biased gene expression in the GTEx liver tissue samples with an FDR-adjusted *p*-value ≤
377 0.1 and absolute $\log_2$ fold-change ≥ 0. N males = 91, N females = 45.

378 **Table S4.** Sex-biased gene expression in the TCGA LIHC tumor-adjacent samples with an FDR-adjusted
379 *p*-value ≤ 0.1 and an absolute $\log_2$ fold-change ≥ 0. N males = 22, N females = 18.

380 **Table S5.** Sex-biased gene expression in TCGA LIHC tumor samples with an FDR-adjusted *p*-value ≤
381 0.01 and an absolute $\log_2$ fold-change ≥ 2. N males = 22, N females = 18.

382 **Table S6.** Differentially expressed genes between matched tumor and tumor-adjacent samples in the
383 combined analysis of male and female samples with an FDR-adjusted *p*-value ≤ 0.01 and an absolute $\log_2$
384 fold-change ≥ 2. N male sample pairs = 22, N female sample pairs = 18.

385 **Table S7.** Differentially expressed genes between matched male tumor and tumor-adjacent samples with
386 an FDR-adjusted *p*-value ≤ 0.01 and an absolute $\log_2$ fold-change ≥ 2. N of sample pairs = 22.

387 **Table S8.** Differentially expressed genes between matched female tumor and tumor-adjacent samples
388 with an FDR-adjusted *p*-value ≤ 0.01 and an absolute $\log_2$ fold-change ≥ 2. N of sample pairs = 18.

389 **Table S9.** Overrepresented GO terms and canonical pathways in the sex-shared tumor vs. tumor-adjacent
390 DEGs. Significant terms and pathways were selected based on an FDR-adjusted *p*-value threshold of
391 0.01.

392 **Table S10.** Overrepresented GO terms and canonical pathways in the male-specific tumor vs. tumor-
393 adjacent DEGs. Significant terms and pathways were selected based on an FDR-adjusted *p*-value
394 threshold of 0.01.

395 **Table S11.** Overrepresented GO terms and canonical pathways in the female-specific tumor vs. tumor-
396 adjacent DEGs. Significant terms and pathways were selected based on an FDR-adjusted *p*-value
397 threshold of 0.01.

398 **Table S12.** *cis*-eQTLs detected in the combined analysis of both sexes. N=367 (N males = 248, N
399 females = 119). Significant eQTLs were selected based on an FDR-adjusted *p*-value threshold 0.01.

400 **Table S13.** *cis*-eQTLs detected in the male-specific analysis. N=248. Significant eQTLs were selected
401 based on an FDR-adjusted *p*-value threshold 0.01.

402 **Table S14.** *cis*-eQTLs detected in the female-specific analysis. N=119. Significant eQTLs were selected
403 based on an FDR-adjusted *p*-value threshold 0.01.

404 **Table S15.** Genomic annotations of eQTLs detected in the combined analysis of both sexes.

405 **Table S16.** Genomic annotations of eQTLs detected in the male-specific analysis.

406 **Table S17.** Genomic annotations of eQTLs detected in the female-specific analysis.

407 **Table S18.** Overrepresented canonical pathways in the male-specific eQTL target genes. Significant
408 terms and pathways were selected based on an FDR-adjusted *p*-value threshold of 0.01.

409 **Table S19.** Top-variants associated with autosomal genes that were expressed in a sex-biased way in
410 HCC tumor samples.

411 Figure Captions

412 **Fig. 1. Patterns of gene expression and molecular etiologies of male and female HCC. A:** Sex-biased
413 gene expression in HCC. A volcano plot of DEGs between male (N=26) and female (N=18) HCC tumor
414 samples. X-linked genes are indicated in pink, Y-linked in green, and autosomal in black. Significant
415 genes were selected based on an FDR-adjusted *p*-value threshold of 0.01 and absolute $\log_2$(FC) threshold
416 of 2. Multiple transcripts of the long non-coding RNA *XIST* are independently expressed. Genes that were
417 not expressed in a sex-biased way in healthy liver (GTEx) or in the tumor-adjacent tissues are indicated
418 with an asterisk. **B:** An example of a gene exhibiting a sex-bias in HCC but not in healthy liver or tumor-
419 adjacent tissues. *DTX1* expression in log(CPM) is shown for male and female samples in each tissue. **C:**
420 A multi-dimensional scaling plot of the paired TCGA LIHC tumor and tumor-adjacent samples of each
421 sex. Euclidean distances between samples were calculated based on 100 genes with the largest standard

422 deviations between samples. Tissue type (dimension 1) and sex (dimension 2) drive the overall patterns of
423 gene expression in HCC. **D:** Venn-diagram of the overlap of DEGs in the sex-specific and combined
424 analysis of matched tumor and tumor-adjacent samples. Substantially more DEGs were identified in the
425 sex-specific analyses. **E:** Sex-specific and sex-shared DEGs were analyzed for the overrepresentation of
426 functional pathways. Sex-specific patterns of pathway enrichment point to differential processes driving
427 the etiology of male and female HCC. **F:** Examples of sex-specific and sex-shared pathways.

428 **Fig 2.** Absolute $\log_2$-fold changes of DEGs detected from tumor vs. tumor-adjacent comparisons in the
429 sex-specific analyses and combined analysis of both sexes. Absolute $\log_2$-fold changes are given for
430 female samples, male samples, and across all samples. Global *p*-values for ANOVA are shown for each
431 DEG type. Adjusted *p*-values based on Kruskal-Wallis tests are shown for each pairwise comparison.

432 **Fig. 3. Sex-specific genetic effects on tumor gene expression in HCC. A:** QQ-plot of eQTL
433 associations in the combined analysis of both sexes (grey), male-specific analysis (blue), and female-
434 specific analysis (red). **B:** Genomic annotations of eQTLs in the combined analysis of both sexes, male-
435 specific analysis, and female-specific analysis. **C:** Overlap of eGenes detected in combined and sex-
436 specific analyses. **D:** An example of a male-specific eQTL. *POGLUT1* expression in tumors is modulated
437 by a germline variant in *cis* in male HCC, but not in female HCC nor in the combined analysis of both
438 sexes, indicating effect modification by sex. Numbers of individuals with each genotype, adjusted
439 significance, and effect size (β) are given for each model.

440 **Fig 4.** Absolute effect sizes of sex-shared and sex-specific eQTLs in males, females, and the whole study
441 sample. Due to the larger sample size, sex-shared low-effect eQTLs are only detected as significant in the
442 combined analysis (A). Sex-shared large effect eQTLs are detected in the combined analysis as well as
443 the sex-specific analyses (B). Sex-specific eQTLs exhibit a larger effect in one sex than the other, and the
444 effect is diluted in the combined analysis (C, D). Sex-shared large effect eQTLs can be detected in sex-
445 specific and combined analyses. Global *p*-values for ANOVA are shown for each eQTL type. Adjusted *p*-
446 values based on Kruskal-Wallis tests are shown for each pairwise comparison.

447 # References

448 1. Clocchiatti A, Cora E, Zhang Y, Dotto GP. Sexual dimorphism in cancer. Nat Rev Cancer.
449 2016;16: 330.

450 2. Bray F, Ferlay J, Soerjomataram I, Siegel RL, Torre LA, Jemal A. Global cancer statistics 2018:
451 GLOBOCAN estimates of incidence and mortality worldwide for 36 cancers in 185 countries. CA Cancer
452 J Clin. 2018; doi:10.3322/caac.21492

453 3. Wisnivesky JP, Halm EA. Sex differences in lung cancer survival: do tumors behave differently
454 in elderly women? J Clin Oncol. 2007;25: 1705–1712.

455 4. OuYang P-Y, Zhang L-N, Lan X-W, Xie C, Zhang W-W, Wang Q-X, et al. The significant
456 survival advantage of female sex in nasopharyngeal carcinoma: a propensity-matched analysis. Br J
457 Cancer. 2015;112: 1554–1561.

458 5. Li CH, Haider S, Shiah Y-J, Thai K, Boutros PC. Sex Differences in Cancer Driver Genes and
459 Biomarkers. Cancer Res. 2018;78: 5527–5537.

460 6. Wands J. Hepatocellular carcinoma and sex. N Engl J Med. 2007;357: 1974–1976.

461 7. Petrick JL, Braunlin M, Laversanne M, Valery PC, Bray F, McGlynn KA. International trends in
462 liver cancer incidence, overall and by histologic subtype, 1978-2007. Int J Cancer. 2016;139: 1534–1545.

463 8. Ladenheim MR, Kim NG, Nguyen P, Le A, Stefanick ML, Garcia G, et al. Sex differences in
464 disease presentation, treatment and clinical outcomes of patients with hepatocellular carcinoma: a single-
465 centre cohort study. BMJ Open Gastroenterol. 2016;3: e000107.

466 9. Gilks WP, Abbott JK, Morrow EH. Sex differences in disease genetics: evidence, evolution, and
467 detection. Trends Genet. 2014;30: 453–463.

468 10. Morrow EH. The evolution of sex differences in disease. Biol Sex Differ. 2015;6: 5.

469 11. Yuan Y, Liu L, Chen H, Wang Y, Xu Y, Mao H, et al. Comprehensive Characterization of
470 Molecular Differences in Cancer between Male and Female Patients. Cancer Cell. 2016;29: 711–722.

471 12. Gong J, Mei S, Liu C, Xiang Y, Ye Y, Zhang Z, et al. PancanQTL: systematic identification of
472 cis-eQTLs and trans-eQTLs in 33 cancer types. Nucleic Acids Res. 2018;46: D971–D976.

473 13. Behrens G, Winkler TW, Gorski M, Leitzmann MF, Heid IM. To stratify or not to stratify: power
474 considerations for population-based genome-wide association studies of quantitative traits. Genet
475 Epidemiol. 2011;35: 867–879.

476 14. Dimas AS, Nica AC, Montgomery SB, Stranger BE, Raj T, Buil A, et al. Sex-biased genetic
477 effects on gene regulation in humans. Genome Res. 2012;22: 2368–2375.

478 15. Grossman RL, Heath AP, Ferretti V, Varmus HE, Lowy DR, Kibbe WA, et al. Toward a Shared
479 Vision for Cancer Genomic Data. N Engl J Med. 2016;375: 1109–1112.

480 16. Webster TH, Couse M, Grande BM, Karlins E, Phung TN, Richmond PA, et al. Identifying,
481 understanding, and correcting technical biases on the sex chromosomes in next-generation sequencing
482 data [Internet]. bioRxiv. 2018. p. 346940. doi:10.1101/346940

483 17. Andrews S. FastQC A Quality Control tool for High Throughput Sequence Data. In:
484 http://www.bioinformatics.babraham.ac.uk/projects/fastqc/ [Internet]. 2010. Available:
485 http://www.bioinformatics.babraham.ac.uk/projects/fastqc/

486 18. Bolger AM, Lohse M, Usadel B. Trimmomatic: a flexible trimmer for Illumina sequence data.
487 Bioinformatics. 2014;30: 2114–2120.

488 19. Kim D, Langmead B, Salzberg SL. HISAT: a fast spliced aligner with low memory requirements.
489 Nat Methods. 2015;12: 357–360.

490 20. Liao Y, Smyth GK, Shi W. featureCounts: an efficient general purpose program for assigning
491 sequence reads to genomic features. Bioinformatics. 2014;30: 923–930.

492 21. McKenna A, Hanna M, Banks E, Sivachenko A, Cibulskis K, Kernytsky A, et al. The Genome
493 Analysis Toolkit: A MapReduce framework for analyzing next-generation DNA sequencing data.
494 Genome Res. 2010;20: 1297–1303.

495 22. DePristo MA, Banks E, Poplin R, Garimella KV, Maguire JR, Hartl C, et al. A framework for
496 variation discovery and genotyping using next-generation DNA sequencing data. Nat Genet. 2011;43:
497 491–498.

498 23. Van der Auwera GA, Carneiro MO, Hartl C, Poplin R, Del Angel G, Levy-Moonshine A, et al.
499 From FastQ data to high confidence variant calls: the Genome Analysis Toolkit best practices pipeline.
500 Curr Protoc Bioinformatics. 2013;43: 11.10.1–33.

501 24. Hinrichs AS, Karolchik D, Baertsch R, Barber GP, Bejerano G, Clawson H, et al. The UCSC
502 Genome Browser Database: update 2006. Nucleic Acids Res. 2006;34: D590–8.

503 25. Robinson MD, McCarthy DJ, Smyth GK. edgeR: a Bioconductor package for differential
504 expression analysis of digital gene expression data. Bioinformatics. 2010;26: 139–140.

505 26. Law CW, Chen Y, Shi W, Smyth GK. voom: precision weights unlock linear model analysis
506 tools for RNA-seq read counts. Genome Biol. 2014;15: R29.

507 27. Xia J, Gill EE, Hancock REW. NetworkAnalyst for statistical, visual and network-based meta-
508 analysis of gene expression data. Nat Protoc. 2015;10: 823–844.

509 28. Leek JT, Storey JD. Capturing Heterogeneity in Gene Expression Studies by Surrogate Variable
510 Analysis. PLoS Genet. 2007;3: e161.

511 29. Stegle O, Parts L, Piipari M, Winn J, Durbin R. Using probabilistic estimation of expression
512 residuals (PEER) to obtain increased power and interpretability of gene expression analyses. Nat Protoc.
513 2012;7: 500–507.

514 30. Zheng X, Levine D, Shen J, Gogarten SM, Laurie C, Weir BS. A high-performance computing
515 toolset for relatedness and principal component analysis of SNP data. Bioinformatics. 2012;28: 3326–
516 3328.

517 31. Delaneau O, Ongen H, Brown AA, Fort A, Panousis N, Dermitzakis E. A complete tool set for
518 molecular QTL discovery and analysis. bioRxiv. 2016; doi:10.1101/068635

519 32. GTEx Consortium. The Genotype-Tissue Expression (GTEx) project. Nat Genet. 2013;45: 580–
520 585.

521 33. Cavalcante RG, Sartor MA. annotatr: genomic regions in context. Bioinformatics. 2017;33:
522 2381–2383.

523 34. Ernst J, Kellis M. ChromHMM: automating chromatin-state discovery and characterization. Nat
524 Methods. 2012;9: 215–216.

525 35. Kukurba KR, Parsana P, Balliu B, Smith KS, Zappala Z, Knowles DA, et al. Impact of the X
526 Chromosome and sex on regulatory variation. Genome Res. 2016;26: 768–777.

527 36. Gaykalova DA, Zizkova V, Guo T, Tiscareno I, Wei Y, Vatapalli R, et al. Integrative
528 computational analysis of transcriptional and epigenetic alterations implicates DTX1 as a putative tumor
529 suppressor gene in HNSCC. Oncotarget. 2017;8: 15349–15363.

530 37. Liu Y, Zheng P. CD24: a genetic checkpoint in T cell homeostasis and autoimmune diseases.
531 Trends Immunol. 2007;28: 315–320.

532 38. Gou Q, Gong X, Jin J, Shi J, Hou Y. Peroxisome proliferator-activated receptors (PPARs) are
533 potential drug targets for cancer therapy. Oncotarget. 2017;8: 60704–60709.

534 39. Mayer IA, Arteaga CL. The PI3K/AKT Pathway as a Target for Cancer Treatment. Annu Rev
535 Med. 2016;67: 11–28.

536 40. Porta R, Borea R, Coelho A, Khan S, Araújo A, Reclusa P, et al. FGFR a promising druggable
537 target in cancer: Molecular biology and new drugs. Crit Rev Oncol Hematol. 2017;113: 256–267.

538 41. Seshacharyulu P, Ponnusamy MP, Haridas D, Jain M, Ganti AK, Batra SK. Targeting the EGFR
539 signaling pathway in cancer therapy. Expert Opin Ther Targets. 2012;16: 15–31.

540 42. Demir IE, Tieftrunk E, Schorn S, Friess H, Ceyhan GO. Nerve growth factor & TrkA as novel
541 therapeutic targets in cancer. Biochim Biophys Acta. 2016;1866: 37–50.

542 43. Zhang Y-L, Wang R-C, Cheng K, Ring BZ, Su L. Roles of Rap1 signaling in tumor cell
543 migration and invasion. Cancer Biol Med. 2017;14: 90–99.

544 44. Choudhry H, Helmi N, Abdulaal WH, Zeyadi M, Zamzami MA, Wu W, et al. Prospects of IL-2
545 in Cancer Immunotherapy. Biomed Res Int. 2018;2018: 9056173.

546 45. Pinho SS, Reis CA. Glycosylation in cancer: mechanisms and clinical implications. Nat Rev
547 Cancer. 2015;15: 540–555.

548 46. Stowell SR, Ju T, Cummings RD. Protein glycosylation in cancer. Annu Rev Pathol. 2015;10:
549 473–510.

550 47. Mehta A, Herrera H, Block T. Chapter Seven - Glycosylation and Liver Cancer. In: Drake RR,
551 Ball LE, editors. Advances in Cancer Research. Academic Press; 2015. pp. 257–279.

552 48. Liang K-H, Yeh C-T. O-glycosylation in liver cancer: Clinical associations and potential
553 mechanisms. Liver Research. 2017;1: 193–196.

554 49. Villegas SN, Gombos R, García-López L, Gutiérrez-Pérez I, García-Castillo J, Vallejo DM, et al.
555 PI3K/Akt Cooperates with Oncogenic Notch by Inducing Nitric Oxide-Dependent Inflammation. Cell
556 Rep. 2018;22: 2541–2549.

557 50. Wang G-L, Iakova P, Wilde M, Awad S, Timchenko NA. Liver tumors escape negative control of
558 proliferation via PI3K/Akt-mediated block of C/EBP alpha growth inhibitory activity. Genes Dev.
559 2004;18: 912–925.

560 51. Huang X, Liu G, Guo J, Su Z. The PI3K/AKT pathway in obesity and type 2 diabetes. Int J Biol
561 Sci. 2018;14: 1483–1496.

562 52. Baar EL, Carbajal KA, Ong IM, Lamming DW. Sex- and tissue-specific changes in mTOR
563 signaling with age in C57BL/6J mice. Aging Cell. 2016;15: 155–166.

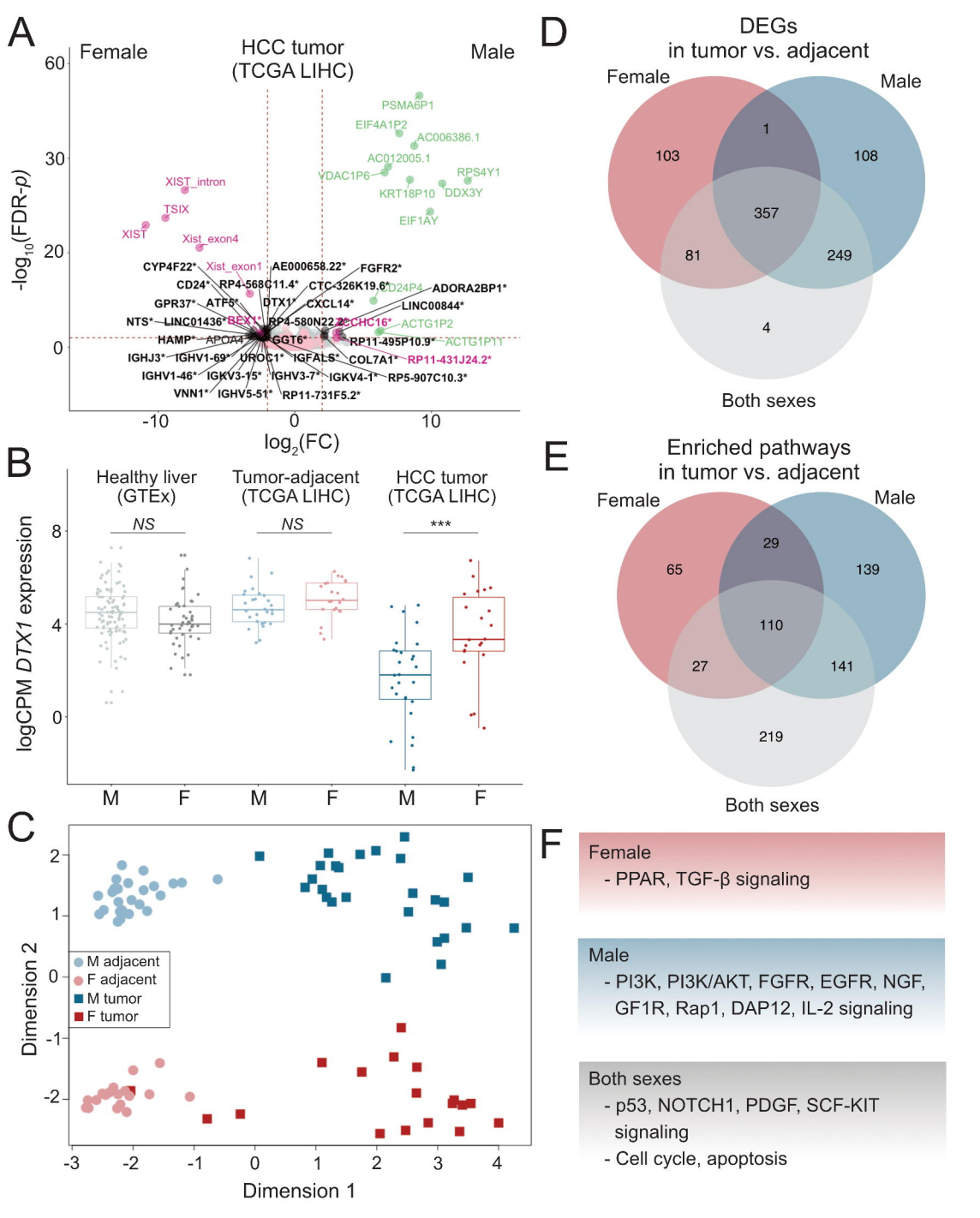
A
Female
HCC tumor
(TCGA LIHC)
Male
-log10(FDR-p)
log2(FC)
PSMA6P1
EIF4A1P2
AC006386.1
AC012005.1
VDAC1P6
RPS4Y1
KRT18P10
DDX3Y
EIF1AY
XIST_intron
TSIX
XIST
Xist_exon4
Xist_exon1
CYP4F22*
AE000658.22*
FGFR2*
CD24*
RP4-568C11.4*
CTC-326K19.6*
ADORA2BP1*
GPR37*
ATF5*
DTX1*
CXCL14*
LINC00844*
NTS*
LINC01436*
BEX1*
RP4-580N22.2*
CHC16*
ACTG1P2
HAMP*
APOA4*
GGT6*
RP11-495P10.9*
ACTG1P11
IGHJ3*
IGHV1-69*
UROC1*
IGFALS*
COL7A1*
RP11-431J24.2*
IGHV1-46*
IGKV3-15*
IGHV3-7*
IGKV4-1*
RP5-907C10.3*
VNN1*
IGHV5-51*
RP11-731F5.2*
B
Healthy liver
(GTEx)
Tumor-adjacent
(TCGA LIHC)
HCC tumor
(TCGA LIHC)
NS
NS
***
logCPM DTX1 expression
M
F
M
F
M
F
C
M adjacent
F adjacent
M tumor
F tumor
Dimension 1
Dimension 2
D
DEGs
in tumor vs. adjacent
Female
Male
103
1
108
357
81
249
4
Both sexes
E
Enriched pathways
in tumor vs. adjacent
Female
Male
65
29
139
110
27
141
219
Both sexes
F
Female
- PPAR, TGF-β signaling
Male
- PI3K, PI3K/AKT, FGFR, EGFR, NGF, GF1R, Rap1, DAP12, IL-2 signaling
Both sexes
- p53, NOTCH1, PDGF, SCF-KIT signaling
- Cell cycle, apoptosis

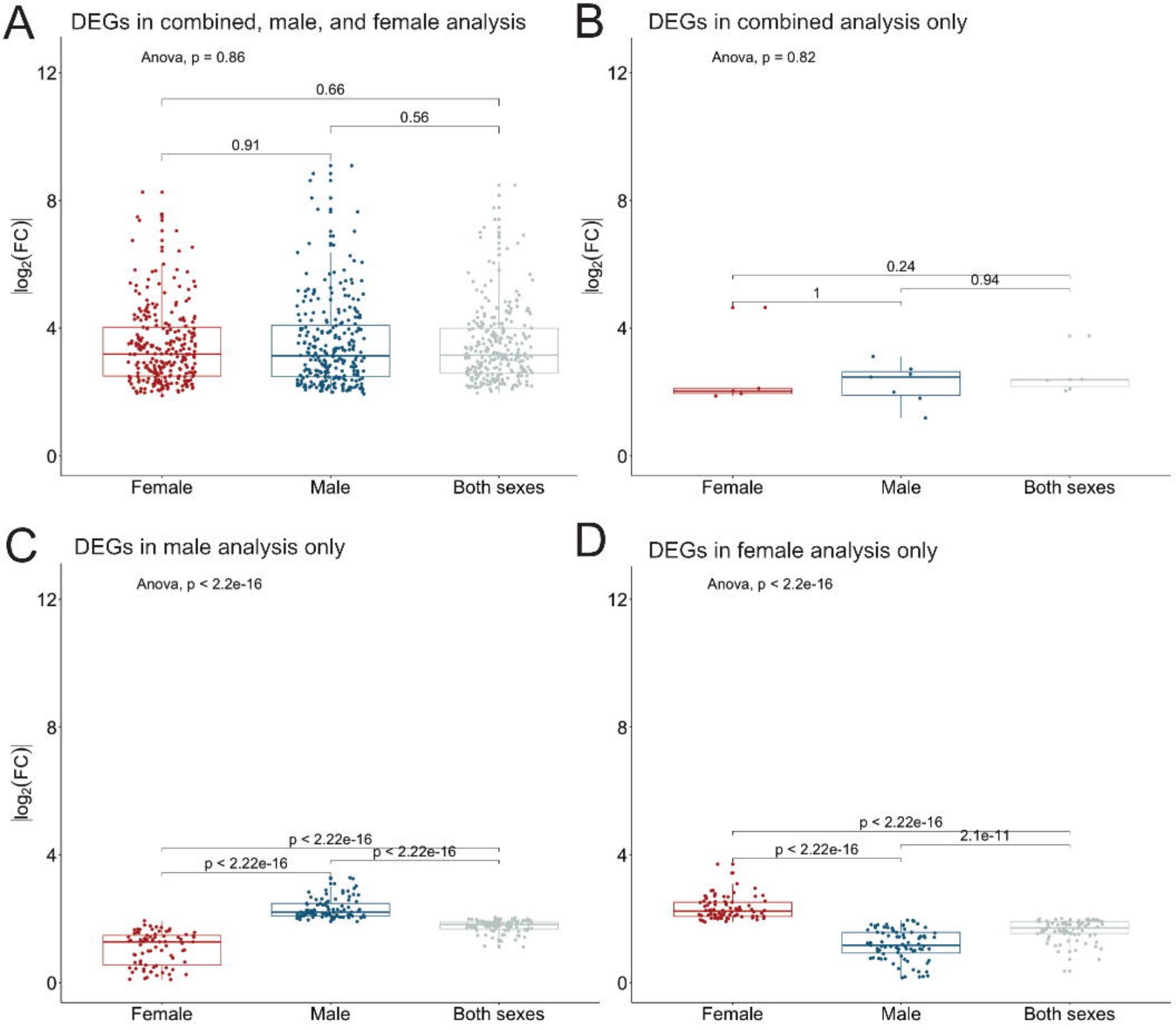
A
DEGs in combined, male, and female analysis
Anova, p = 0.86
0.66
0.56
0.91
|log2(FC)|
Female
Male
Both sexes
B
DEGs in combined analysis only
Anova, p = 0.82
0.24
0.94
1
C
DEGs in male analysis only
Anova, p < 2.2e-16
p < 2.22e-16
p < 2.22e-16
p < 2.22e-16
D
DEGs in female analysis only
Anova, p < 2.2e-16
p < 2.22e-16
2.1e-11
p < 2.22e-16

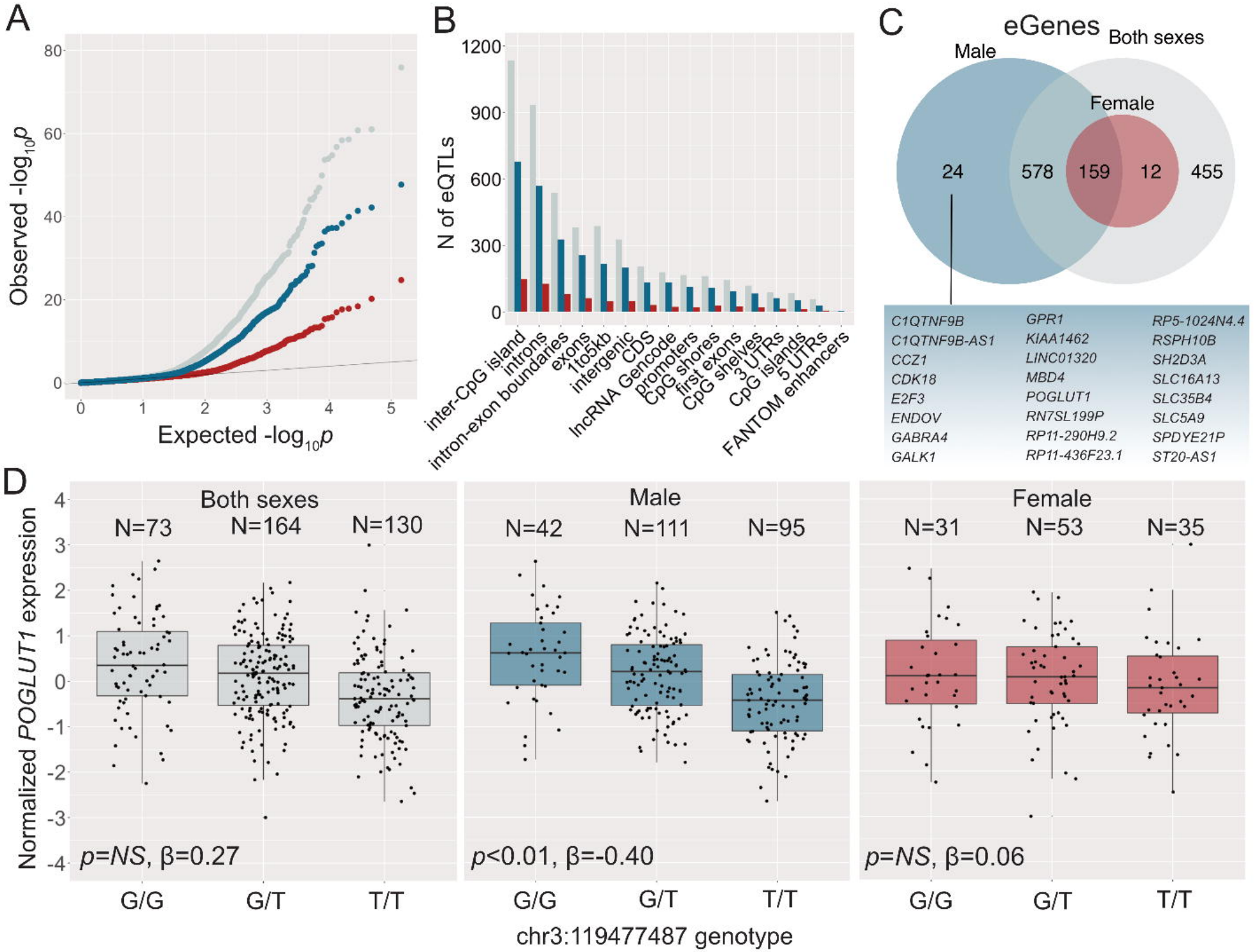
A
Observed -log10p
Expected -log10p
B
N of eQTLs
inter-CpG island
introns
intron-exon boundaries
exons
1to5kb
intergenic
CDS
lncRNA Gencode
promoters
CpG shores
first exons
CpG shelves
3 UTRs
CpG islands
5 UTRs
FANTOM enhancers
C
eGenes
Male
Both sexes
Female
24
578
159
12
455
C1QTNF9B
C1QTNF9B-AS1
CCZ1
CDK18
E2F3
ENDOV
GABRA4
GALK1
GPR1
KIAA1462
LINC01320
MBD4
POGLUT1
RN7SL199P
RP11-290H9.2
RP11-436F23.1
RP5-1024N4.4
RSPH10B
SH2D3A
SLC16A13
SLC35B4
SLC5A9
SPDYE21P
ST20-AS1
D
Normalized POGLUT1 expression
Both sexes
N=73
N=164
N=130
p=NS, β=0.27
Male
N=42
N=111
N=95
p<0.01, β=-0.40
Female
N=31
N=53
N=35
p=NS, β=0.06
G/G
G/T
T/T
chr3:119477487 genotype

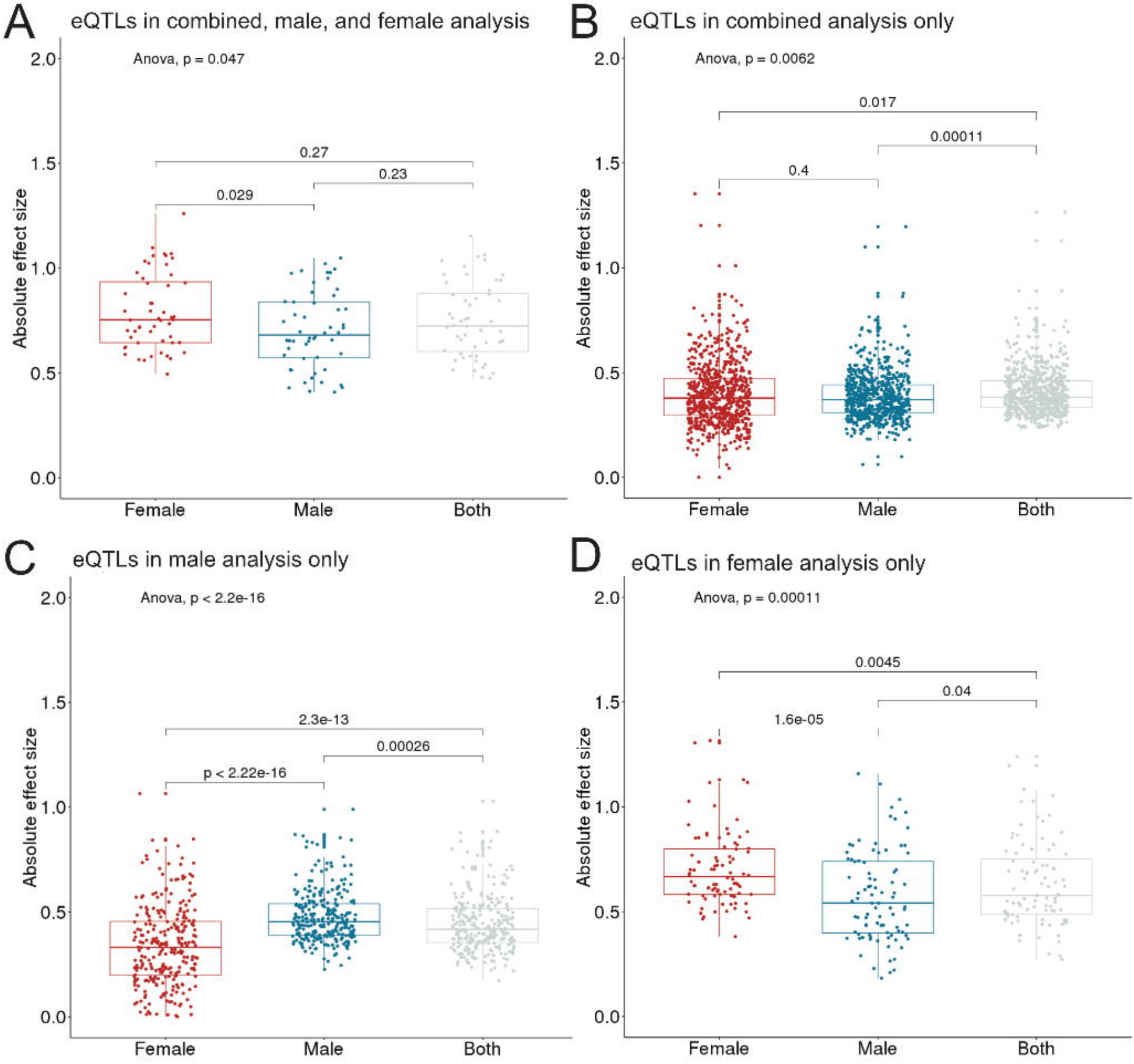
A
eQTLs in combined, male, and female analysis
Anova, p = 0.047
0.27
0.23
0.029
Absolute effect size
2.0
1.5
1.0
0.5
0.0
Female
Male
Both
B
eQTLs in combined analysis only
Anova, p = 0.0062
0.017
0.00011
0.4
Absolute effect size
2.0
1.5
1.0
0.5
0.0
Female
Male
Both
C
eQTLs in male analysis only
Anova, p < 2.2e-16
2.3e-13
0.00026
p < 2.22e-16
Absolute effect size
2.0
1.5
1.0
0.5
0.0
Female
Male
Both
D
eQTLs in female analysis only
Anova, p = 0.00011
0.0045
0.04
1.6e-05
Absolute effect size
2.0
1.5
1.0
0.5
0.0
Female
Male
Both

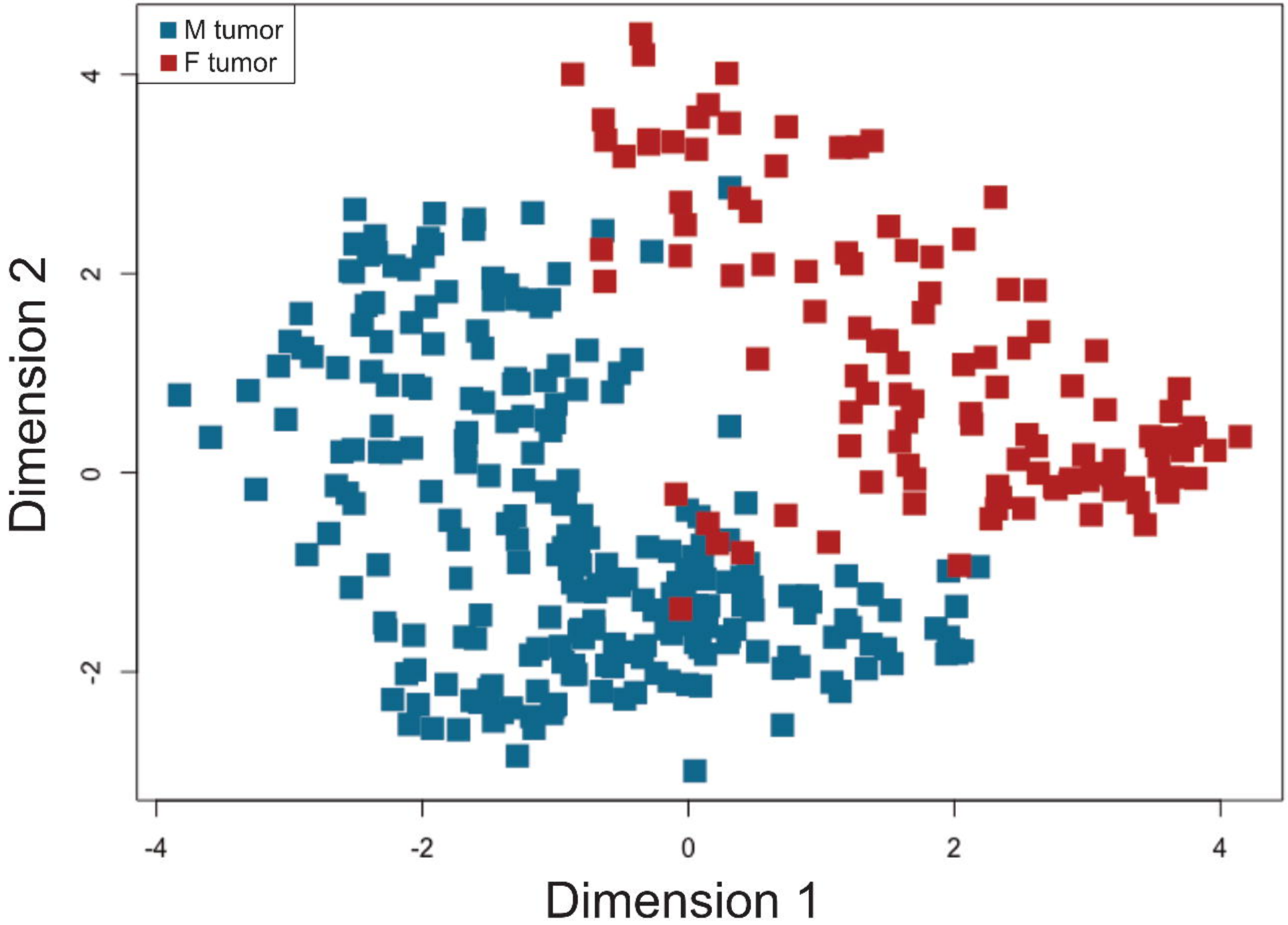
M tumor
F tumor
Dimension 2
Dimension 1
4
2
0
-2
-4
-2
0
2
4

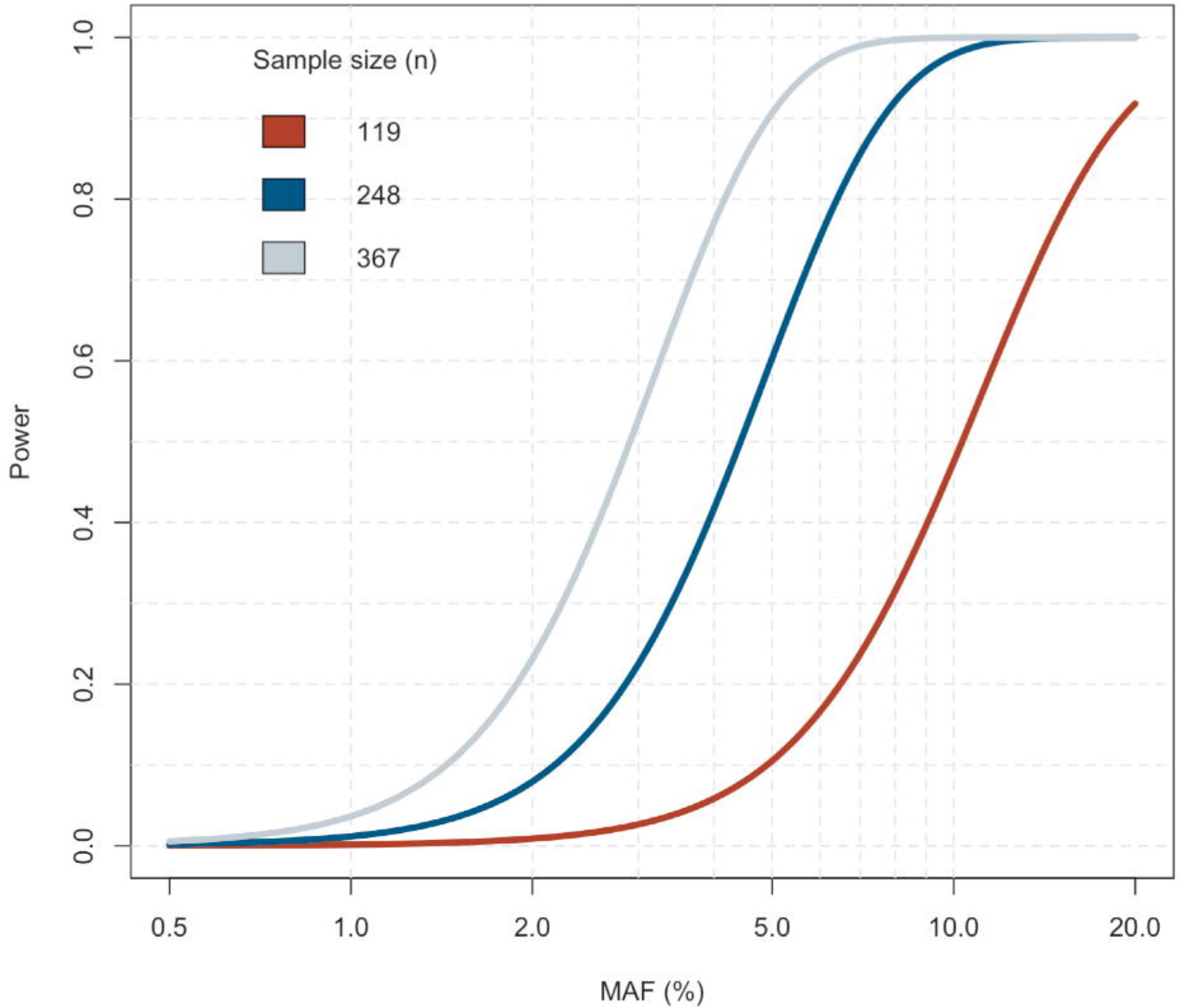
Sample size (n)
119
248
367
Power
0.0
0.2
0.4
0.6
0.8
1.0
0.5
1.0
2.0
5.0
10.0
20.0
MAF (%)